ACS APPLIED BIO MATERIALS Article
Cite This: ACS Appl. Bio Mater. 2019, 2, 4941−4952
www.acsabm.org

Improvement of Production and Isolation of Human Neuraminidase-1 *in Cellulo* Crystals

Kotaro Koiwai,[†] Jun Tsukimoto,[‡] Tetsuya Higashi,[‡] Fumitaka Mafuné,[§] Ken Miyajima,[§] Takanori Nakane,[∥] Naohiro Matsugaki,[†] Ryuichi Kato,[†,⊥] Serena Sirigu,[#] Arjen Jakobi,[▽,○,◆] Matthias Wilmanns,[▽] Michihiro Sugahara,[¶] Tomoyuki Tanaka,[¶,●] Kensuke Tono,[¶,◇] Yasumasa Joti,[¶,◇] Makina Yabashi,[¶,◇] Osamu Nureki,[∥] Eiichi Mizohata,[■,□] Toru Nakatsu,[▲] Eriko Nango,[¶,●] So Iwata,[¶,●] Leonard M. G. Chavas,[#] Toshiya Senda,[†,⊥] Kohji Itoh,[*,‡] and Fumiaki Yumoto[*,†]

[†]Structural Biology Research Center, Photon Factory, Institute of Materials Structure Science, High Energy Accelerator Research Organization, 1-1 Oho, Tsukuba, Ibaraki 305-0801, Japan

[‡]Department of Medicinal Biotechnology, Institute for Medicinal Research, Graduate School of Pharmaceutical Science, Tokushima University, Tokushima 770-8501, Japan

[§]Department of Basic Science, School of Arts and Sciences, The University of Tokyo, Komaba, Meguro, Tokyo 153-8902, Japan

[∥]Department of Biological Sciences, Graduate School of Science, The University of Tokyo, 7-3-1 Hongo, Bunkyo-ku, Tokyo 113-0033, Japan

[⊥]School of High Energy Accelerator Science, SOKENDAI University, Tsukuba, Ibaraki 305-0801, Japan

[#]PROXIMA-1, Synchrotron SOLEIL, BP 48, L'Orme des Merisiers, 91192 Gif-sur-Yvette, France

[▽]Hamburg Unit c/o DESY, European Molecular Biology Laboratory (EMBL), Notkestrasse 85, 22607 Hamburg, Germany

[○]Structural and Computational Biology Unit, European Molecular Biology Laboratory (EMBL), Meyerhofstrasse 1, 69117 Heidelberg, Germany

[◆]Department of Bionanoscience, Delft University of Technology, Van der Maasweg 9, 2629 HZ Delft, The Netherlands

[¶]RIKEN SPring-8 Center, 1-1-1 Kouto, Sayo-cho, Sayo-gun, Hyogo 679-5148, Japan

[●]Department of Cell Biology, Graduate School of Medicine, Kyoto University, Yoshidakonoe-cho, Sakyo-ku, Kyoto 606-8501, Japan

[◇]Japan Synchrotron Radiation Research Institute, 1-1-1 Kouto, Sayo-cho, Sayo-gun, Hyogo 679-5198, Japan

[■]Department of Applied Chemistry, Graduate School of Engineering, Osaka University, 2-1 Yamadaoka, Suita, Osaka 565-0871, Japan

[□]Japan Science and Technology Agency, PRESTO, 4-1-8 Honcho, Kawaguchi, Saitama 332-0012, Japan

[▲]Graduate School of Pharmaceutical Sciences, Kyoto University, Sakyo, Kyoto 606-8501, Japan

Supporting Information

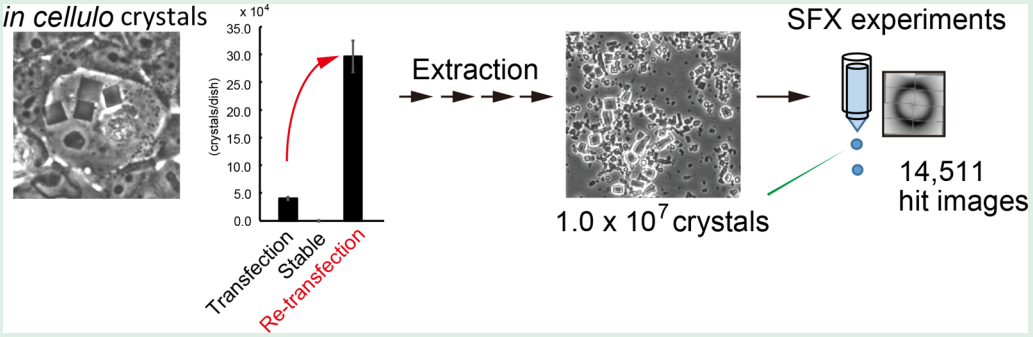

ABSTRACT: *In cellulo* crystallization is a developing technique to provide crystals for protein structure determination, particularly for proteins that are difficult to prepare by *in vitro* crystallization. This method has a key advantage: it requires neither a protein purification step nor a crystallization step. However, there is still no systematic strategy for improving the
continued...

Received: July 30, 2019
Accepted: October 7, 2019
Published: October 7, 2019

DOI: 10.1021/acsabm.9b00686
ACS Appl. Bio Mater. 2019, 2, 4941−4952

technique of *in cellulo* crystallization because the process occurs spontaneously. Here we report a protocol to produce and extract *in cellulo* crystals of human lysosomal neuraminidase-1 (NEU1) in human cultured cells. Overexpression of NEU1 protein by the retransfection of cells pretransfected with *neu1*-overexpressing plasmid improved the efficiency of NEU1 crystallization. Microscopic analysis revealed that NEU1 proteins were not crystallized in the lysosome but in the endoplasmic reticulum (ER). Screening of the buffer conditions used to extract crystals from cells further improved the crystal yield. The optimal pH was 7.0, which corresponds to the pH in the ER. Use of a high-yield flask with a large surface area also yielded more crystals. These optimizations enabled us to execute a serial femtosecond crystallography experiment with a sufficient number of crystals to generate a complete data set. Optimization of the *in cellulo* crystallization method was thus shown to be possible.

KEYWORDS: *in cellulo crystallization, human neuraminidase-1, X-ray free electron laser, serial femtosecond crystallography, transmittance electron microscopy, endoplasmic reticulum, protein overexpression*

INTRODUCTION

Crystallizations are routinely performed *in vitro* in protein crystallography to determine the three-dimensional structure of macromolecules or complexes and ultimately the molecular mechanism of their functions. However, proteins can also be crystallized *in vivo*.[1] *In vivo* crystallizations of proteins in humans and silkworms were first reported in the middle of the 19th century.[2−4] The first such crystals in humans were named Charcot−Leyden crystals, and in 1995, these were shown to be composed of galectin-10 protein.[5] The crystals in silkworm with polyhedrosis were later shown to be *Bombyx mori* nucleopolyhedrovirus.[6,7] Since these early reports, *in vivo* crystallizations have been observed in many species from bacteria to humans. For example, crystallizations in *Escherichia coli* RecA,[8] *Bacillus thuringiensis* Cry3A,[9] *Paramecium* trichocyst,[10] yeast alcohol oxidase (AOX),[11,12] cockroach, *Diploptera punctate*, lipocalin-milkprotein (Lili-Mip),[13] and human eosinophil major basic protein (EMBP)[14] have been reported. Crystal growth has also been observed in cultured cells; in this study, we use the term *in cellulo* crystals to refer to the crystals produced in cultured cell lines, to distinguish them from the *in vivo* crystals produced in nature. Submicron crystals of *Trypanosoma brucei* cathepsin B,[15,16] trypanosomal inosine monophosphate dehydrogenase (IMPDH),[16] *B. mori* cypovirus 1 polyhedron,[17] human immunoglobulin G (IgG),[18] fluorescence protein Xpa,[19] and a catalytic domain of PAK4[20] have been reported as *in cellulo* crystals.[1] Because *in cellulo* crystallization has the advantage of requiring neither the protein purification nor crystallization step, it has been actively adopted and improved; the various technical developments include the use of polyhedrin to facilitate *in cellulo* crystallization[21] and a procedure from sample preparation to data collection for the *in cellulo* crystals.[17] Therefore, *in cellulo* crystallization can now be used for proteins that are difficult to purify and crystallize *in vitro*. Human neuraminidase-1 (NEU1) is a difficult protein to purify in a homogeneous state for the structure determination by *in vitro* crystallization; recombinant NEU1 expressed in bacterial cells is insoluble, and recombinant NEU1 expressed in insect cells is in a heterogeneous oligomeric state.[22]

Neuraminidases (EC 3.2.1.18), also known as sialidases, are hydrolytic enzymes and have the ability to digest terminal sialic acids of glycans. They are widely distributed from microorganisms and viruses to mammals.[23] One of the neuraminidases, NEU1, is synthesized in the endoplasmic reticulum (ER) and subsequently transported to the Golgi apparatus, and then to the lysosome.[24] In these cellular compartments, NEU1 is sequentially modified by glycosides. For the transportation and neuraminidase activity in the lysosomes, NEU1 requires interaction with an NEU1-interacting protein, cathepsin A.[24] In humans, amino-acid substitutions of NEU1 are known to be related to lysosomal diseases such as sialidosis[25] and galactosialidosis.[26] Structural determination of NEU1 has been attempted to clarify the molecular mechanisms by which mutations on the *neu1* gene render it functionally deficient. While *in cellulo* crystallization of NEU1 has been reported,[22] there have been few basic investigations to characterize the molecular structure of NEU1 in the last two decades. One exception was a study in which serial femtosecond crystallography (SFX) was applied to *in cellulo* crystals.[27] However, the number of diffraction images in that report was too small to constitute a complete data set for structure determination. Therefore, improvement of the yield of *in cellulo* crystals was required to realize the structure determination.

Here we report that it is possible to improve the number of human NEU1 proteins crystallized *in cellulo*. Overexpression of the *neu1* gene and selection of the transfected cells increased the number of *in cellulo* crystals in human embryonic kidney (HEK) 293FT cells. Transmission electron microscopy (TEM) analysis of NEU1-overexpressing cells revealed that NEU1 proteins were not crystallized in the lysosomes but rather in the ER. Screening of the extraction conditions to concentrate the crystals by reducing contaminating cell debris and nucleic acids enabled us to execute an SFX experiment with a sufficient number of isolated *in cellulo* crystals. The diffraction images revealed the large lattice parameters of the crystals and their heterogeneity. This illustrates the inherent difficulty of structural determination of NEU1 even when using *in cellulo* crystals.

EXPERIMENTAL SECTION

Cell Culture and Transfection. Human embryonic kidney (HEK) 293FT cells (Thermo Fischer Scientific, Waltham, MA) were cultured in Dulbecco's modified Eagle's medium (DMEM) (Wako Pure Chemical Industries, Osaka, Japan) supplemented with 10% (v/v) fetal bovine serum (FBS) (Biosera, Kansas City, MO) in 5% CO_2. For transfection, confluent cells on a 10 cm dish were transfected with 20 μg of pCXhygro-neu1 or pCXhygro-neu1-His plasmid in lipofectamine 3000 (Thermo Fischer Scientific) and Opti-MEM Reduced Serum medium, GlutaMAX (Thermo Fischer Scientific), and the medium was changed after 20−24 h. HEK 293FT cells expressing NEU1 (293FT_neu1) were selected with 200 μg/mL hygromicin B (Nacalai Tesque, Kyoto, Japan). Expression of the NEU1 protein was confirmed by Western blotting using a rabbit polyclonal antihuman NEU1 antibody (catalogue number (cat. no.): 100-401-396) (Rockland Immunochemicals, Limerick, PA) as a primary antibody coupled to a horseradish peroxidase (HRP)-conjugated antirabbit Ig (cat. no.: NA934-1 ML) (GE Healthcare, Little Chalfont, UK) as a secondary antibody, and an ImageQuant LAS 3000 mini imaging system (GE Healthcare). β-Tubulin as an internal control was detected by using mouse anti-β-tubulin (cat. no.: 014-25041) (Wako Pure Chemical Industries) and HRP-conjugated antimouse IgG antibodies (cat. no.: NXA931-1 ML) (GE Healthcare). For SFX experiments, 293FT cells harboring crystals were cultured in two Hyperflask M cell culture vessels (Corning, Corning, NY) with a surface area of 1720 cm^2/flask

DOI: 10.1021/acsabm.9b00686
ACS Appl. Bio Mater. 2019, 2, 4941−4952

that required addition of 550 mL of medium to transport the cultured cells safely and efficiently. Together, the two flasks contained 3.0×10^8 cells. The cells in the flasks were transported to a beamline of SACLA and incubated at 37 °C until being processed just before the SFX experiments.

Extraction of NEU1 Crystals from Mammalian Cells. After discarding the medium, cells were lysed on a 10 cm dish in 10 mL of Buffer 1 (25 mM HEPES-NaOH, 150 mM NaCl, 0.1% (v/v) Triton X-100, pH 7.0). The cell lysate was pipetted over 5 strokes with a mechanical pipet. Crystals thus extracted from the cells were harvested by centrifugation at 3000 *g* using a swing-type rotor (Hitachi T4SS31; Hitachi, Tokyo) for a centrifuge (Hitachi HimacCF 16RX; Hitachi). Crystals were washed in 5 mL of Buffer 2 (25 mM HEPES-NaOH, 150 mM NaCl, pH 7.0), and suspended in 10 mL of Buffer 3 (25 mM HEPES-NaOH, 1.0 M NaCl, pH 7.0). For the biochemical and single crystal X-ray experiments, a buffer containing 25 mM HEPES-NaOH, 1.0 M NaCl, 0.1 mg/mL DNase I (Wako Pure Chemical Industries), and 0.1 mg/mL RNase A (Wako Pure Chemical Industries) at pH 7.0 was defined as Buffer 4. DNA and RNA were digested by shaking at 37 °C for 30 min. Large debris was removed by careful pipetting before filtering by passing the crystal solution through 30 μm pores. Crystals were manually counted using a hemocytometer (Biomedical Science, Tokyo) placed under a microscope.

For the SFX experiments, the protocol for the large-scale extraction of crystals from the Hyperflask M (Corning) was adjusted as follows. To reduce contamination by debris in the final product, the HEK 293FT cells were washed in 200 mL of phosphate-buffered saline (PBS) (10 mM KH_2PO_4-Na_2HPO_4, 137 mM NaCl, 2.7 mM KCl, pH 7.4) in a Hyperflask M, lysed in 300 mL of Buffer 1, suspended in 35 mL of Buffer 2, and resuspended in 35 mL of Buffer 4 containing 25 mM HEPES-NaOH, 1.0 M NaCl, 1.0 mg/mL DNase I and 1.0 mg/mL RNase A at pH 7.0. Crystals over $10 \times 10 \times 2$ μm^3 in size were concentrated by centrifugation at 3000 *g* to $\sim 2.0 \times 10^7$ crystals/mL, and the final volume was adjusted to 500 μL with Buffer 3. Twenty μL of 10 mg/mL DNase I and RNase A dissolved in Buffer 3 was added at a concentration of 1 mg/mL to prevent clogging of the droplet injector nozzle.

Immunostaining and Confocal Laser Fluorescence Microscopy. HEK 293FT cells transfected with pCXhygro-neu1 were fixed in 4% paraformaldehyde and permeabilized with 50% (v/v) methanol in PBS. After blocking by 5% (w/v) goat serum and 1% (w/v) BSA, the cells were immunoreacted by a mixture of primary antibodies containing a mouse anti-NEU1 antibody (cat. no.: sc-166824) (Santa Cruz Biotechnology, Dallas, TX) and a rabbit anti-Calnexin (C5C9) antibody (cat. no.: 2679P) (Cell Signaling Technology, Danvers, MA) or a rabbit anti-LAMP1 antibody (cat. no.: ab24170) (Abcam, Cambridge, UK), stained with 5 μg/mL Hoechst33258 (Merck, Darmstadt, Germany), and immunoreacted by a mixture of secondary antibodies containing FITC-labeled antimouse IgG (cat. no.: ab47830) (Abcam) and Cy3-labeled antirabbit IgG (cat. no.: 111-165-006) (Jackson ImmunoResearch, West Grove, PA) antibodies. After washing, the cells were stored in an observation solution (50% (v/v) glycerol, 0.26% (w/v) diazabicyclo(2,2,2)octane) and observed under a Zeiss LSM 700 Axio Observer confocal laser microscope (Carl Zeiss Microscopy GmbH, Jena, Germany). Hoechst33258, FITC, and Cy3 were excited using 405, 488, and 555 nm wavelength laser lines, respectively. Fluorescences of 405−490 nm from Hoechst33258, 490−565 nm from FITC, and 565−720 nm from Cy3 were independently detected. Images were obtained using ZEN lite software (Carl Zeiss Microscopy GmbH).

Transmission Electron Microscopy. TEM analyses were performed at Tokai Electron Microscopy (Nagoya, Japan). The HEK 293FT_neu1 cells constructed in this study (see the Optimization of the Timing of Cell Culture to Produce the Required Amount of NEU1 *in cellulo* Crystals section) were transfected with *neu1*-plasmid and cultured for 4 days on a 3 cm dish. After washing directly on the dish with PBS, the cells were sequentially fixed in Solution-1 (100 mM PBS, 2% (w/v) paraformaldehyde, 2% (w/v) glutaraldehyde, pH 7.4), Solution-2 (100 mM PBS, 2% (w/v) glutaraldehyde, pH 7.4), and Solution-3 (100 mM PBS, 2% (w/v) osmium tetroxide, pH 7.4). The fixed cells were dehydrated with ethanol, embedded with a Quetol-812 resin (EMJapan, Tokyo), and sectioned in ultrathin layers down to 70 nm using an ultramicrotome. Sections were stained first with 2% (w/v) uranyl acetate and then with lead stain (Sigma-Aldrich, St. Louis, MO). Observations were recorded at 80 kV using a transmission electron microscope equipped with a CCD camera (JEM-1400Plus, JEOL, Tokyo). The images were fast Fourier-transformed with ImageJ2 software[28] before analyses.

SFX Experiments and analyses. Two batches of NEU1 crystals were prepared for the SFX experiments; each batch was prepared using two flasks. One batch of crystals was extracted 2 days before the beamtime in order to investigate the effect of the time from extraction to beamtime on the quality of the crystals. The other batch of crystals was extracted from just before the SFX beamtime. SFX experiments were performed at SACLA, beamline 3 experimental hutch 2,[29] using 7.0 keV X-rays with a pulse duration of <10 fs and a repetition rate of 30 Hz. The pulse energy at the sample position was ~430 μJ per pulse at the beamtime. A droplet injector was used in the SFX experiments for sample injection because it requires a much smaller amount of crystals for structural determination (approximately 1.0×10^7 diffractive crystals).[30] The droplet injector was installed on the Diverse Application Platform for Hard X-ray diffraction in SACLA (DAPHNIS).[31] The droplet injector in the SFX experiments was operated under the following conditions: a combination of 90 V for head amplitude and 50 μs for duration of an electric pulse, 80 V and 60 μs, or 50 V and 60 μs. The parameters were occasionally changed according to the form of the droplets. The X-ray free electron laser (XFEL) beam was focused to a beam diameter of 1.5 μm in fwhm by Kirkpatrick−Baez mirrors. Diffraction patterns were recorded using a multiport CCD detector with eight sensor modules[32] at a sample-to-detector distance of 50 mm. Images were first filtered for possible hits by using a Cheetah-based online processing system,[33,34] and auto-indexed using CrystFEL (version 0.6.2) and DirAx.[35,36] Diffraction images were output for visual inspection by the *hdfsee* viewer in the CrystFEL program suite. Some images were exported from *hdfsee* to the ADSC format and displayed in the Adxv program (http://www.scripps.edu/tainer/arvai/adxv.html) to analyze interspot distances.

Single Crystal X-ray Experiment. NEU1 crystals were prepared on a small scale. The crystals were soaked in a buffer containing 25 mM HEPES-NaOH, 1.0 M NaCl, and 30% glycerol. The crystals were scooped by a cryo-loop containing multiple crystals, then loop mounted, and quenched in liquid nitrogen. Diffraction of the crystals was measured under cryo-conditions at 100 K with a wavelength of 1.00000 Å and exposure time of 0.5 s at the synchrotron beamline BL41XU at SPring-8 (Japan Synchrotron Radiation Research Institute, Hyogo, Japan) using a PILATUS3 6 M detector (DECTRIS, Baden, Switzerland).

Biochemical Analyses. Biochemical analyses were performed on crystals washed with a buffer containing 25 mM HEPES-NaOH and 300 mM NaCl at pH 7.0 and solubilized in a buffer containing 25 mM HEPES-NaOH and 20 mM NaCl at pH 7.0. Digestion of glycoside by endoglycosidases, Endo Hf and PNGase F, was performed as described by the manufacturer (New England BioLabs, Ipswich, MA). Proteins were fractionated by sodium dodecyl sulfate (SDS)-polyacrylamide gel electrophoresis (PAGE) and detected by silver staining, Coomassie brilliant blue (CBB) staining or Western blotting using a rabbit polyclonal antihuman NEU1 antibody and an HRP-conjugated antirabbit IgG antibody as described in the Cell Culture and Transfection section.

RESULTS AND DISCUSSION

Producing NEU1 *in Cellulo* Crystals in a Mammalian Cell Line. To perform an SFX experiment for structure determination, over 1.0×10^7 diffractive crystals should be prepared.[37] Previous SFX experiments using NEU1 *in cellulo* crystals of size $1 \times 1 \times 1$ μm^3 performed at SACLA resulted in a very low hit rate or no hits at all. The mean hit rate was approximately 0.2%, and there was only a single diffraction image with 3.0 Å resolution among the 200 diffraction images

DOI: 10.1021/acsabm.9b00686
ACS Appl. Bio Mater. 2019, 2, 4941−4952

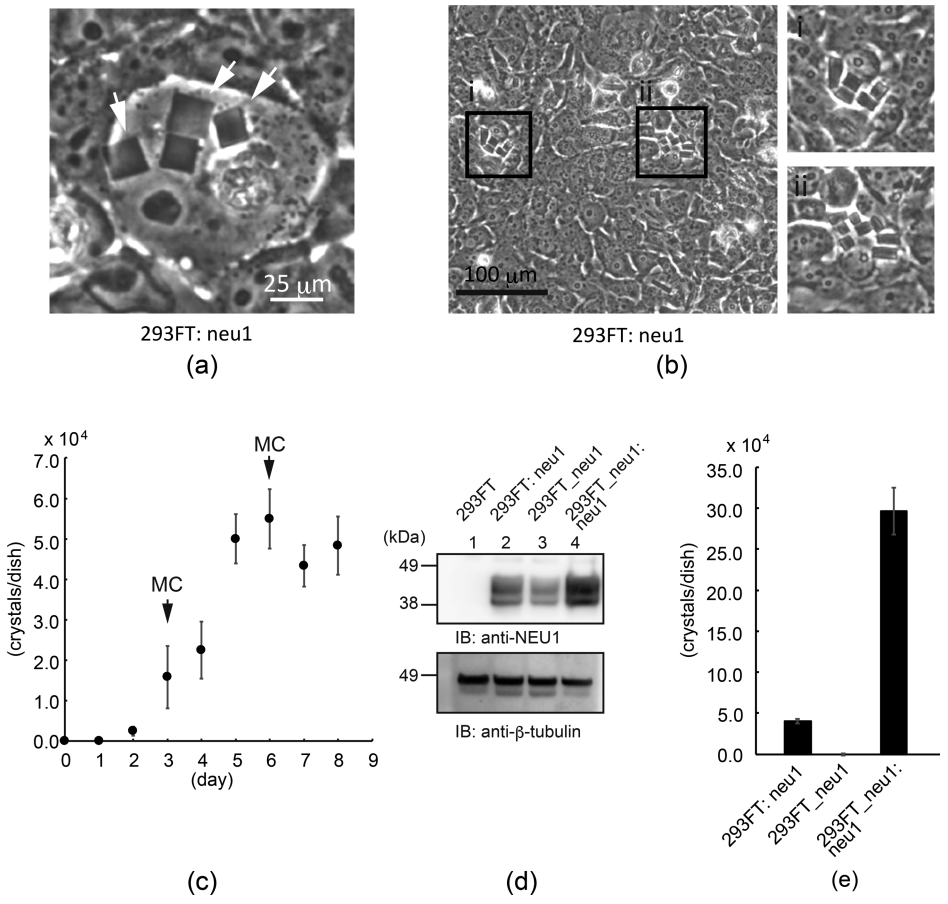

Figure 1. Production of NEU1 *in cellulo* crystals. (a, b) Crystal morphology and NEU1 crystal-production efficiency. HEK 293FT cells were transiently transfected with an *neu1*-coding plasmid (293FT: neu1). At 4 days after the transfection, cells were observed under a phase contrast microscope. The field with the highest production efficiency of NEU1 *in cellulo* crystals is shown. The scale bar represents 100 μm. Two of the cells with crystals were enlarged (i, ii), and their shape was mainly rectangular. (c) Growth curve of the number of NEU1 crystals in HEK 293FT cells. After transfection, cells were harvested and lysed on the indicated days. Crystals were roughly extracted and counted under microscopy. The medium was changed on days 3 and 6 after transfection (medium change, MC). Error bars indicate standard error, calculated from a triplicate assay. (d) NEU1 expression in the used cell lines. Cells were lysed with sonication and denatured by boiling in SDS-sample buffer. Twenty μg of whole cell proteins extracted from 293FT cells, 293FT: neu1 cells, 293FT: neu1 cells selected with hygromycin B (293FT_neu1), and 293FT_neu1 cells transiently transfected again (293FT_neu1: neu1) was fractionated by SDS-PAGE and analyzed with Western blotting analysis. NEU1 and β-tubulin as an internal control were immunoreacted using an anti-NEU1 antibody and anti-β-tubulin antibody, respectively. IB indicates immunoblotting. (e) Improvement of the production efficiency of NEU1 crystals. Crystals were extracted from 293FT: neu1, 293FT_neu1, or 293FT_neu1: neu1 cells 5 days after transfection and counted under a microscope. Error bars indicate standard error, calculated from a triplicate assay.

collected.[27] The study indicated that a much higher concentration of diffractive NEU1 crystals would be required for the protein structural determination. Next, therefore, we sought to improve the protocol for the production and extraction of NEU1 crystals.

First, the production of *in cellulo* crystals was re-examined. HEK 293FT cells were transfected with a *neu1*-overexpressing plasmid, pCXhygro-neu1, using a lipofection method reported previously (Figure 1a).[22,27] Because it was hard to count the *in cellulo* crystals within the cells that were cultured to over 100% confluence on the plate, we decided to evaluate the yield of the crystals as the number of the crystals obtained from a 10 cm-culture dish with a 55 cm^2 culture area after the extraction.

Second, the production of *in cellulo* crystals was evaluated using five mammalian cell lines: HEK 293FT cells in order to follow the previous study,[27] *GNTI* gene-deficient HEK 293S cells in order to improve the quality of the crystals by making the glycosylation state of NEU1 proteins in the lysosome identical, human fibroblast T1 cells from a patient with galactosialidosis who exhibited no cathepsin A (CTSA) activity[38,39] in order to evaluate whether transportation of NEU1 from the ER to the lysosome by CTSA affects the quantity of crystals, human epithelioid cervix carcinoma HeLa cells, and a Chinese hamster ovary (CHO) cell line (Supporting Information Table S1). On the fifth day after the transfection, crystals were produced in all of the cell lines. Among them, HEK 293FT and 293S cells yielded approximately 5.0×10^4 crystals in 100 μL of PBS containing 0.1% (v/v) Triton X-100 in a 10 cm dish, representing an approximately 2-fold greater efficiency than the other cell lines. The size of the crystals was not significantly different among the cell lines. The HEK 293S cells also exhibited similar efficiency for *in cellulo* crystallization of NEU1, and the resulting crystals had similar morphology as those produced by the HEK 293FT cells. Based on the results of the previous study,[27] we selected HEK 293FT cells for further analysis in our present experiments.

Size and Morphology of NEU1 *in Cellulo* Crystals. There has been no investigation into whether the size of NEU1 *in cellulo* crystals is sufficient for diffraction in an SFX experiment. In a previous report, a $1 \times 1 \times 1$ μm^3 area of NEU1 crystals (the

DOI: 10.1021/acsabm.9b00686
ACS Appl. Bio Mater. 2019, 2, 4941−4952

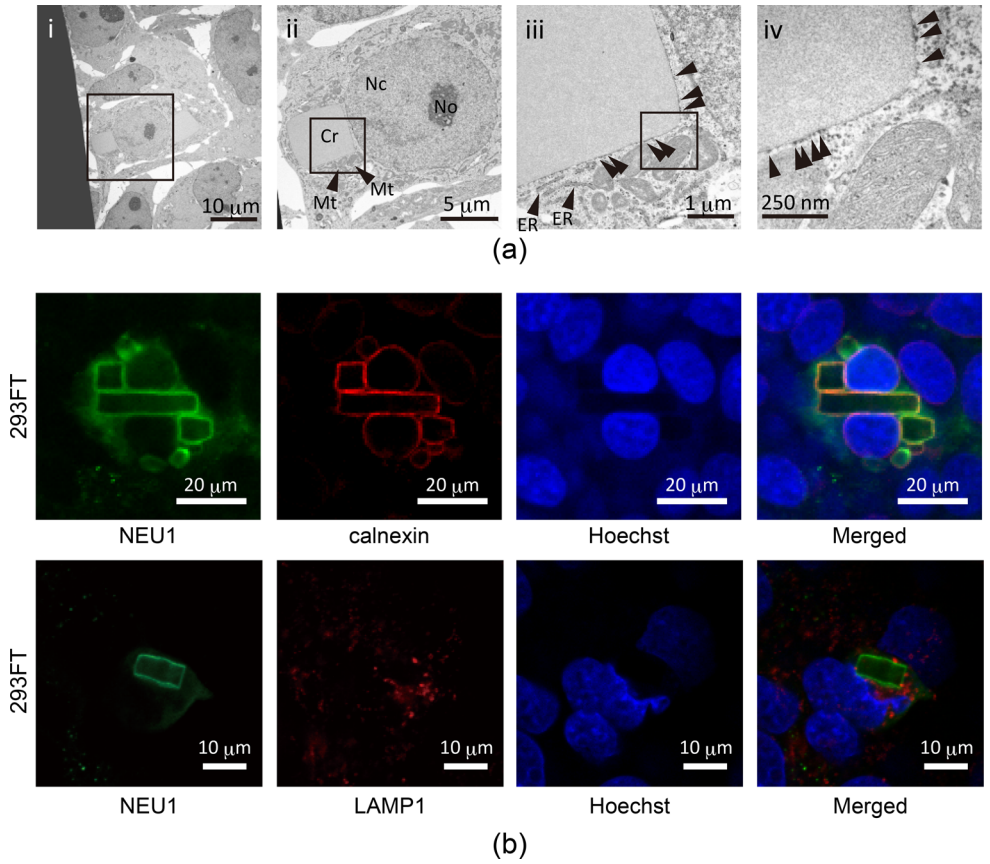

Figure 2. NEU1 *in cellulo* crystals localize in the ER. (a) (i–iv) Localization of the NEU1 crystals in cells using TEM analysis. HEK 293FT cells producing NEU1 crystals were fixed with paraformaldehyde, glutaraldehyde, and osmium tetroxide. The fixed cells were embedded in a resin, ultrathin-sectioned to 70 nm, and negatively stained. Regions indicated by squares are enlarged. (ii) Cellular compartments and the NEU1 crystals are labeled as followed: Nc, nucleus; No, nucleolus; ER, endoplasmic reticulum; Mt, mitochondrion; and Cr, crystal. (iii, iv) Arrowheads indicate ribosomes. (b) Localization of NEU1 *in cellulo* crystals using immunostaining. HEK 293FT cells overexpressing NEU1 were fixed, permeabilized, stained by Hoechst33258 (blue; Hoechst), and immunoreacted with the following antibodies as primary antibodies: anti-NEU1 (green, NEU1), anticalnexin as an ER marker (red in an upper panel, calnexin), and anti-LAMP1 as a lysosome marker (red in a lower panel, LAMP1). As secondary antibodies, FITC-coupled (green) and Cy3-coupled (red) antibodies were used. Images of each fluorescence were independently captured by a confocal laser scanning microscope and merged (Merged) using Zen lite software.

actual number of crystals was not described in the study) was applied for an SFX experiment, resulting in a 0.2% hit rate,[27] suggesting that most of the NEU1 crystals were not hit. Based on a study showing that ~5 μm of high-quality lysozyme crystals were diffracted up to 2.3 Å resolution with the current system at the SACLA beamline,[30] we aimed to prepare NEU1 crystals longer than 10 μm to raise the possibility of the XFEL-beam hitting the crystals in an SFX experiment.

Using a transfection method described in the previous study,[27] we observed that there were mainly two types of crystals in the cells. In the cells of approximately 50 × 50 × 10 μm^3 in size, the first type was the flat plate-type crystals which were approximately 10 × 10 × 2 μm^3 in size (Figure 1a) and approximately 20 × 20 × 2 μm^3 in size at the maximum. The second type were the long rectangular crystals which were approximately 2 × 2 × 20 μm^3 in size (Figure 1b) and approximately 2 × 2 × 50 μm^3 in size at the maximum. The length of each type of crystals varied from 1 to 50 μm (Figure 1b). The crystals were observed over the 5 days following transfection. We attempted to enlarge the NEU1 *in cellulo* crystals by culturing for 9 days on the same dish, but we could not produce significantly larger crystals. Therefore, we decided to prepare ca. 1.0×10^7 crystals with >10 μm length.

Optimization of the Timing of Cell Culture to Produce the Required Amount of NEU1 *in cellulo* Crystals. The appropriate timing for isolation of *in cellulo* crystals from HEK 293FT cells cultured on a 10 cm dish was investigated to maximize the number of isolated crystals with low contamination by debris. Cells with crystals could not be transferred to another dish for new passage because the cells died after producing the crystals. The production of crystals was saturated on the fifth day after transfection (Figure 1c). Further culture led to more contamination by debris and higher viscosity, which might have been due to contamination by cellular nucleic acids. Therefore, the fifth day was selected as the harvesting time.

In the case of NEU1 crystallization in the HEK 293FT cell line, approximately 5.0×10^4 crystals were obtained from a 10 cm dish on the fifth day after transient transfection (Figure 1c), indicating that 200 dishes of 10 cm diameter would be required to obtain 1.0×10^7 crystals for SFX data collection. Since this was not a reasonable number of dishes to handle in an experiment, it was necessary to improve the number of crystals produced per dish.

In a 10 cm dish, theoretically, 8.8×10^6 cells can be cultured at 100% confluency, indicating that at most only 0.6% of cells produced crystals. One of the reasons for this low rate was that many nontransfected cells remained. Therefore, the cells

DOI: 10.1021/acsabm.9b00686
ACS Appl. Bio Mater. 2019, 2, 4941–4952

transfected with pCXhygro-neu1 harboring a hygromycin B-resistance gene were selected under an antibiotic condition with 200 μg/mL hygromycin B (HyB). Even though the HyB-selected 293FT cells (hereafter referred to as HEK 293FT_neu1 cells) overexpressed NEU1, no crystal was observed at 1 week after passage (Figure 1d,e). Under the assumption that the NEU1-expression level in each cell contributed to the production of crystals, we concluded that enhancing the level of NEU1 overexpression in individual cells would lead to more efficient production of NEU1 crystals. To induce a higher level of NEU1-overexpression, HEK 293FT_neu1 cells were transiently transfected again with the pCXhygro-neu1 plasmid. As expected, NEU1-overexpressing retransfectants produced about 3.0×10^5 crystals per 10 cm dish (Figure 1d,e). Theoretically, 3.4% of the retransfectants produced from one to several crystals in each cell. This was an approximately 6-fold increase compared to the case of transient overexpression. In order to overexpress NEU1 more, we transfected the plasmid again (for a total of three transfections), but the cells died before producing the crystals.

Since the cells died after producing *in cellulo* crystals, it was impossible to establish a cell line that consistently produced a large number of NEU1 crystals. Cell death with *in cellulo* crystals has been observed in the case of cells with Charcot-Leyden crystals.[40] Such cell death is a problem to be overcome in *in cellulo* crystallography. Therefore, we invented a retransfection method, in which the pCXhygro-neu1 plasmid was transfected into NEU1-overexpressing cells that had already been transfected with the same plasmid. Such retransfection is the best way to increase the number of crystals at the moment.

Localization of NEU1 *in Cellulo* Crystals Using TEM and CLSM. In the previous report on NEU1 *in cellulo* crystallization for an SFX experiment, the NEU1 crystals were maintained with cell lysate and PBS (pH 7.4) buffer.[27] We thought that this condition could be further improved for the NEU1 crystals, because NEU1 has been recognized as a lysosomal protein, which exists in an acidic environment.[24,41]

The location of the crystals was investigated with TEM and confocal laser scanning microscopy (CLSM). Cells holding NEU1 crystals were fixed, ultrathin-sectioned, negatively stained, and observed using TEM. The analysis revealed that the NEU1 crystals were enveloped by membrane (Figure 2a(iii)). There was no space between the crystals and the membrane in any of the observed cells. Interestingly, ribosomes appeared as dots over the membrane in the magnified image (Figure 2a(iii,iv)). These observations suggest that NEU1 crystals were produced in the rough ER, not in the lysosome. The localization of NEU1 crystals was also analyzed with coimmunostaining using a CLSM with the marker protein calnexin for the ER[42] and the marker protein LAMP1 for the lysosome.[43] The results confirmed that the NEU1 crystals were localized in the ER (Figure 2b), which was consistent with the previous observation.[44] This suggested that the NEU1 *in cellulo* crystals might be stable in a buffer with a pH of 7.0, which is the pH in the ER.[45]

In addition to the localization of the NEU1 protein composing the crystals in the ER, none of the overexpressed and uncrystallized NEU1 detected by immunostaining was localized in the lysosome. We speculated that this was because endogenous cathepsin A, which transports NEU1 from the ER to the lysosome,[24] could not deliver all of the NEU1 molecules. This could have resulted in an accumulation of NEU1 proteins in the ER.

Extraction of NEU1 *in Cellulo* Crystals. An extraction step was necessary because at most only 3.4% of the retransfectants could produce NEU1 *in cellulo* crystals. The crystals must be concentrated into an injector to obtain a reasonable hit rate of X-ray irradiation to crystals during the SFX experiment. To deliver the crystals to the X-ray irradiation area without clogging the nozzle, it was necessary to remove cell debris and nucleic acids from the solution containing the crystals. Hence, the extraction procedure was composed of four steps: (1) cell lysis, (2) removal of detergent, (3) disruption of the cellular nuclei, and (4) removal of genomic DNA or RNA.

The conditions related to the detergent, pH, and salt concentration in the lysis buffer were optimized to produce a buffer that could be used for the purification and storage without dissolving the crystals before the beamtime. The initial lysis buffer contained PBS (pH 7.4) and 0.05% Triton X-100 (Tx-100) to break the cellular membranes. The NEU1 crystals dissolved in the lysis buffer within 1 h. To investigate whether Tx-100 made the crystals dissolve, the buffer was exchanged by centrifugation and resuspension in PBS (pH 7.4) without Tx-100. The crystals could be stored for 1 day after the crystal extraction, indicating that the detergent made the crystals dissolve and should be removed immediately. However, these crystals dissolved in 3 days (Figure 3a), suggesting that the solution could be improved further. Then, various pH values, ranging from pH 5.0 to 9.0, were screened for the buffer at 4 °C with an NaCl concentration of 150 mM. The NEU1 crystals were kept in a buffer composed of 25 mM HEPES-NaOH and 150 mM NaCl at pH 7.0, which corresponds to the pH in the ER, for 5 days (Figure 3b). The crystals were also stored for 5 days in a phosphate buffer with a pH of 7.0. The effect of NaCl concentrations of 100, 150, 300, 500, or 1000 mM in a buffer containing 25 mM HEPES-NaOH at pH 7.0 on the stability of the NEU1 crystals was examined. Although the crystals were stored over 5 days in buffers with NaCl concentrations higher than 500 mM, the combination of the higher NaCl concentration and 0.05% Tx-100 induced dissolution of the crystals. After these experiments, the optimal lysis buffer was determined to be Buffer 1, which was composed of 25 mM HEPES-NaOH, 150 mM NaCl, and 0.05% or 0.1% Tx-100 at pH 7.0 for small- or large-scale preparations, respectively. It was consistent that the pH of this buffer was within the pH range in the ER.[45] Buffer 2, which was composed of 25 mM HEPES-NaOH and 150 mM NaCl at pH 7.0, was used to remove the detergent in the second step. To store the crystals at this step, the Buffer 2 should be exchanged to a buffer containing more than 300 mM NaCl.

Disruption of the cellular nuclei at the third step was necessary to realize a sufficient concentration of crystals for the SFX experiments (Figure 3c); otherwise the suspension of crystals would contain a large quantity of nuclei, and such coexistence of crystals and nuclei would lead to a lower hit rate in the XFEL diffractions from crystals. We found that the nuclei were disrupted and the cellular nucleic acids formed sticky debris in a buffer containing 1.0 M NaCl and 25 mM HEPES-NaOH at pH 7.0. The NEU1 *in cellulo* crystals could be stored for 2 weeks in the buffer at 4 °C. Thus, the optimal buffer was determined to be Buffer 3, which is composed of 25 mM HEPES-NaOH and 1.0 M NaCl at pH 7.0.

At the fourth step, genomic DNA and RNA were removed. Since genomic DNA formed large, sticky debris after the treatment with Buffer 3, the debris was roughly removed using a pipet in the large-scale preparation. Then, DNase I and RNase A

DOI: 10.1021/acsabm.9b00686
ACS Appl. Bio Mater. 2019, 2, 4941−4952

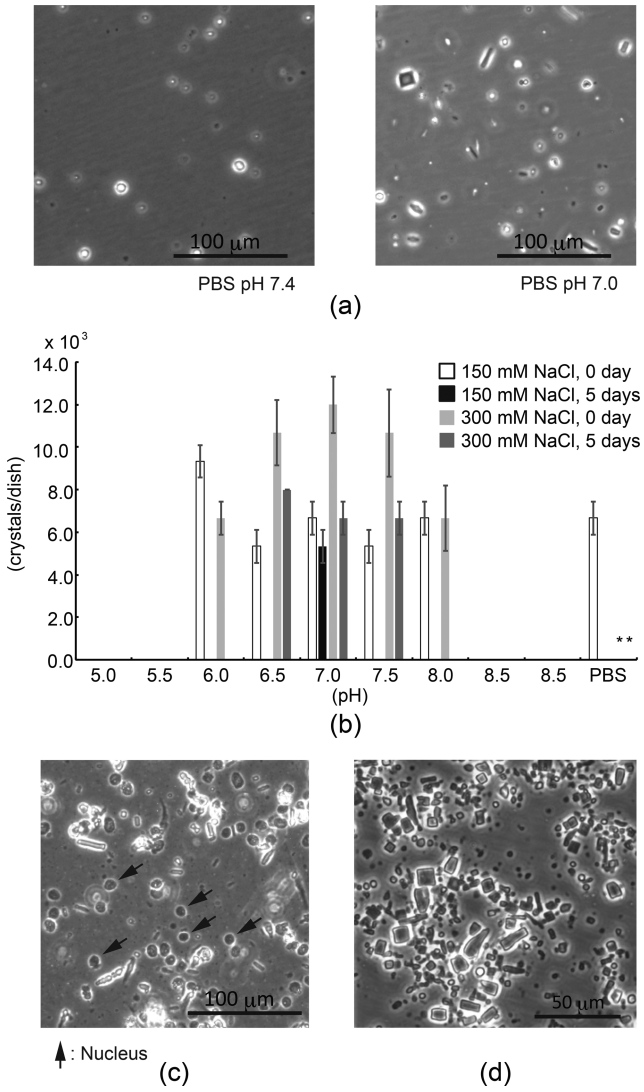

Figure 3. Extraction of NEU1 protein from *in cellulo* crystals. (a) Crystal stability in PBS at pH 7.4 or at pH 7.0. Cells were lysed in PBS containing Tx-100 and stored in PBS without Tx-100 at 4 °C. At 3 days after extraction, crystals were observed under a phase contrast microscope. (b) Crystal stability in buffers with different pH and NaCl concentration. Cells were lysed in PBS with Tx-100 at pH 7.0 and stored in the indicated buffers without Tx-100 containing 150 mM or 300 mM NaCl. The pH of the buffers was adjusted as indicated: from pH 5.0 to pH 5.5 for 25 mM acetate buffer, from pH 6.0 to pH 6.5 for 25 mM MES-NaOH buffer, from pH 7.0 to pH 7.5 for 25 mM HEPES-NaOH buffer, from pH 8.0 to pH 8.5 for 25 mM Tris-HCl buffer, and pH 9.0 for 25 mM Glycine-NaOH buffer. Crystals were counted with a hemocytometer under a phase contrast microscope. PBS containing 300 mM NaCl was not examined (asterisks, *). (c) The crystal suspension contains nuclei as debris. Cells were lysed in PBS containing Tx-100 and observed under a phase contrast microscope. Arrows indicate nuclei. (d) Purified NEU1 *in cellulo* crystals. NEU1 crystals were extracted from 293FT cells. The crystals were applied to a hemocytometer and observed under a phase contrast microscope.

were added to digest the residual genomic DNA and RNA at the fourth step. The digestion by 0.1 mg/mL DNase I and RNase A at 37 °C for 1 h was sufficient for the small-scale preparation, whereas 1 mg/mL of the nucleases was added for the large-scale preparation. The remaining debris could be removed by filtration using a 100 μm mesh-size filter after pipetting. Using this protocol, approximately 1.0×10^5 crystals with a size of over $10 \times 10 \times 1$ μm^3 were obtained from a 10 cm dish (Figure 3d). Therefore, the optimal buffer was determined to be Buffer 4 (25 mM HEPES-NaOH, 1.0 M NaCl, 0.1 mg/mL DNase I, and 0.1 mg/mL RNase A at pH 7.0 for small-scale preparation, or 25 mM HEPES-NaOH, 1.0 M NaCl, 1 mg/mL DNase I, and 1 mg/mL RNase A at pH 7.0 for large-scale preparation). This buffer was exchanged with Buffer 3 for storage to remove the nucleases. For the SFX experiment, Buffer 4 was exchanged with a new one to prevent clogging in the droplet injector nozzle during the experiment.

To increase crystals from a reasonable volume of cell culture instead of using hundreds of dishes for the SFX beamtime, two Hyperflask M cell culture vessels (Corning) were used for the cell culture. These flasks were selected because of their large surface area of 1720 cm^2/flask. A volume of 550 mL of medium was required to minimize shaking with air during transportation of the sample. The two flasks contained 3.0×10^8 cells, theoretically harboring over 5.0×10^6 crystals, with 1.0×10^7 crystals being required for an SFX experiment. Two batches of the two flasks were prepared to investigate the effect of the time from extraction to the beamtime on the quality of the crystals; one was for preparation of crystals just before the beamtime, and the other was for preparation 2 days before the beamtime.

Thus, we established a procedure to extract NEU1 *in cellulo* crystals from cells with high purity using four buffers. In order to obtain a high yield of crystals, one of the essential parameters was pH. Because the NEU1 crystals were localized in the ER, we adjusted the pH to 7.0. It might be possible to apply this same pH to other *in cellulo* crystals growing in the ER, but the pH should be changed for *in cellulo* crystals growing at other cellular locations. To prevent the NEU1 crystals from dissolving, Buffer 1 should be changed to Buffer 2, which did not contain detergent. In contrast, the stability of some crystals is not affected by detergent. For such crystals, the step of changing Buffer 1 to Buffer 2 can be omitted. To concentrate the NEU1 crystals, the cellular nuclei were disrupted by treatment with Buffer 3, and the nucleic acids were digested by nucleases in Buffer 4. In the case of crystals composed of nucleic acid-interacting proteins, these buffers may destabilize the crystals.

Characterization of NEU1 *in Cellulo* Crystals. With the protocol for the NEU1 *in cellulo* crystallization and extraction in hand, we proceeded to biochemically characterize the NEU1 protein. The NEU1 crystals were dissolved in a buffer containing 25 mM HEPES-NaOH and 20 mM NaCl at pH 7.0 and fractionated by SDS-PAGE. Western blotting on the solubilized NEU1 crystals revealed a 40 kDa protein (Figure 4a), indicating that the *in cellulo* crystals were composed of only NEU1 protein.

In the ER, nascent proteins are modified by glycoside whose first *N*-acetylglucosamine residue from the proteins is not fucosylated, and the glycoside is fucosylated in the Golgi apparatus after transportation from the ER to the Golgi apparatus. NEU1 is known to be glycosylated at Asn186, Asn343, and Asn352.[44,46] To evaluate the glycosylation, the dissolved NEU1 protein was digested by two endoglycosidases, Endo Hf, which can digest glycosides without the fucosylation, and PNGase F, which can digest glycosides both with/without the fucosylation, under native and denatured conditions (shown as "native" or "denatured" in Figure 4b, respectively). The observed molecular weight shifted down to 36 kDa after digestion by both of the glycosidases, suggesting that the NEU1 protein in the crystals was glycosylated, but the innermost *N*-acetylglucosamine residue of the glycoside was not fucosylated. Despite the digestion of glycoside with the glycosidases, the

DOI: 10.1021/acsabm.9b00686
ACS Appl. Bio Mater. 2019, 2, 4941−4952

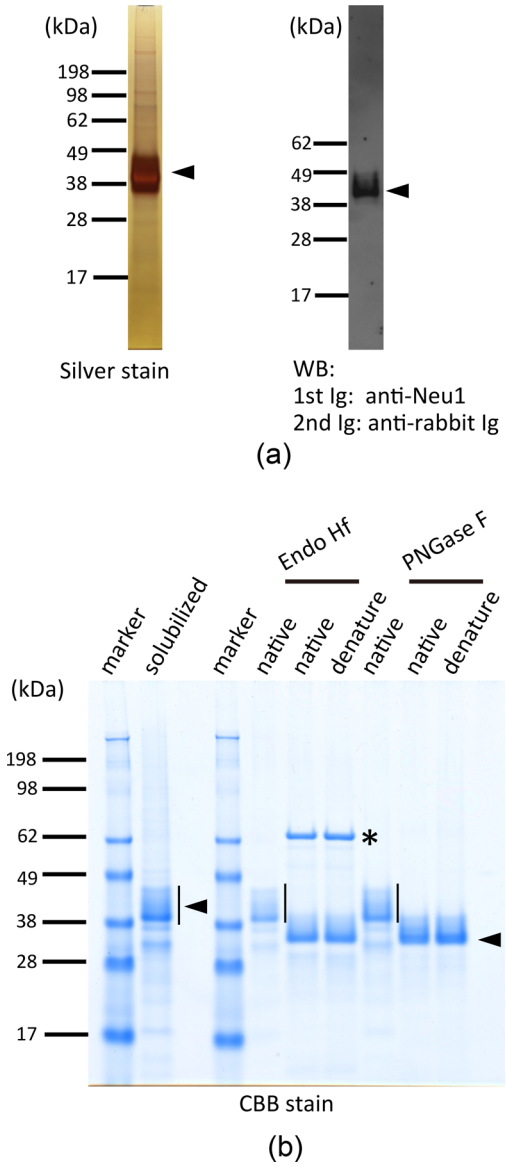

Figure 4. NEU1 *in cellulo* crystals are composed of glycosylated NEU1 protein. *In cellulo* crystals of NEU1 were extracted and solubilized in a buffer containing 25 mM HEPES-NaOH and 20 mM NaCl at pH 7.0. NEU1 proteins were fractionated to evaluate their properties in SDS-PAGE analyses and stained with silver staining. They were also analyzed by Western blotting using anti-NEU1 antibody as a primary antibody (first Ig) and HRP-conjugated antirabbit antibody as a secondary antibody (second Ig) (a). The molecular weight of the marker is indicated in kilodaltons (kDa). Arrows indicate the position of the NEU1 protein. (b) The NEU1 protein (native) or boiled NEU1 polypeptide (denatured) was mixed with Endo Hf or PNGase F endoglycosidases. Proteins were fractionated by SDS-PAGE and stained by CBB staining. Bars, arrowheads, and asterisks indicate heterogeneously glycosylated NEU1 proteins and NEU1 proteins digested by endoglycosidases and Endo Hf, respectively. The molecular weight of the marker is indicated in units of kDa.

bands of the NEU1 proteins in SDS-PAGE remained to be smeared, suggesting that the NEU1 proteins were heterogeneous because of other post-translational modifications.

SFX Analysis of NEU1 *in Cellulo* Crystals. At the SACLA beamline 3, ~1.0×10^7 crystals that were larger than 10 μm were extracted from the two flasks just before the beamtime (batch_1), and the same numbers of crystals from the flasks 2 days before the beamtime (batch_2), and the crystals were added to 500 μL of Buffer 4 (Figure 5a). At the XFEL beamtime at the SACLA from November 27 to 28 in 2015, 14,511 diffraction images from batch_1 and 410 diffraction images from batch_2 were collected over 6 h of injection by a droplet injector.[30] The hit rate of batch_1 was 3.5%, calculated from the Cheetah- and CrystFEL-based pipeline in the SACLA.[34] The maximum observed resolution of the diffraction spots was 8 Å, which was as high as that from crystals extracted with a previous method. The unit cell constants could not be determined with CrystFEL. Manual examination of the images revealed that the diffraction spots were tightly packed on the detector, which corresponded to real space vectors of approximately 1200 Å length (Figure 5b,c). The lengths of the unit cell vectors were estimated to be roughly 100−200 Å, 300−500 Å, and 1100−1300 Å by manual measurement of the diffraction images on Adxv. Some of the diffraction patterns were similar to those observed in the previous study,[27] which was also observed in an experiment at the synchrotron (Supporting Information Figure S1). Due to the low resolutions of the diffraction images, the unit cell vector parallel to the beam was not well-defined. One of the lengths of the unit cell parameters, 100−200 Å, correlated with that of the TEM analysis. The low resolution of the X-ray diffraction images and poor results of the fast Fourier-transform (FFT) analysis of the TEM images were consistent (Figure 5d).

The cause of the poor quality of the crystals may have been heterogeneity of the NEU1 molecules. Because the glycoside was cleaved by both of the glycosidases (Figure 4b) and the crystals were localized in the ER, a type of glycoside might be high-mannose type. In humans, there are various patterns of high-mannose-type glycoside. We speculated that the heterogeneous glycosylation state caused the heterogeneity. To inhibit the glycosylation, we incorporated the Ala mutation onto the Asn352 residue. However, we could not determine whether the heterogeneity was attributable to the heterogeneous glycosylation state because the Asn352Ala mutant was not produced in the cells (Supporting Information Figure S2). The result was not consistent with the previous study. This may have been due to further improvements in the production of the NEU1 proteins that were expressed in the HEK293-6E cell line and cultured by a suspension method with the result that the proteins expressed exceeded the number of proteins degraded. However, the heterogeneity appeared to remain even though the mutant was crystallized in the previous study.

In terms of improving the crystal quality, one approach is to optimize the cell culture methods. In this study, the NEU1 crystals were grown in adherent cells, while in a previous study they were grown in suspended cells.[44] Crystals in the adherent cells were likely to be pressed against the cellular membranes. Thus, the crystal growth could be affected by such pressure. In addition to optimizing the cell culture methods, another means of improving the crystal quality is to treat the extracted crystals with one or more chemical compounds; post-crystallization treatment with soaking in carefully formulated solutions has been shown to improve crystal quality *in vitro*.[47] The improvement of the crystal quality should be the next challenge in *in cellulo* crystallography.

CONCLUSION

In cellulo crystallography using mammalian cells is a developing method. A protocol for *in cellulo* crystallization of human NEU1 was established after optimization of the production and extraction of the crystals (Figure 6).

DOI: 10.1021/acsabm.9b00686
ACS Appl. Bio Mater. 2019, 2, 4941−4952

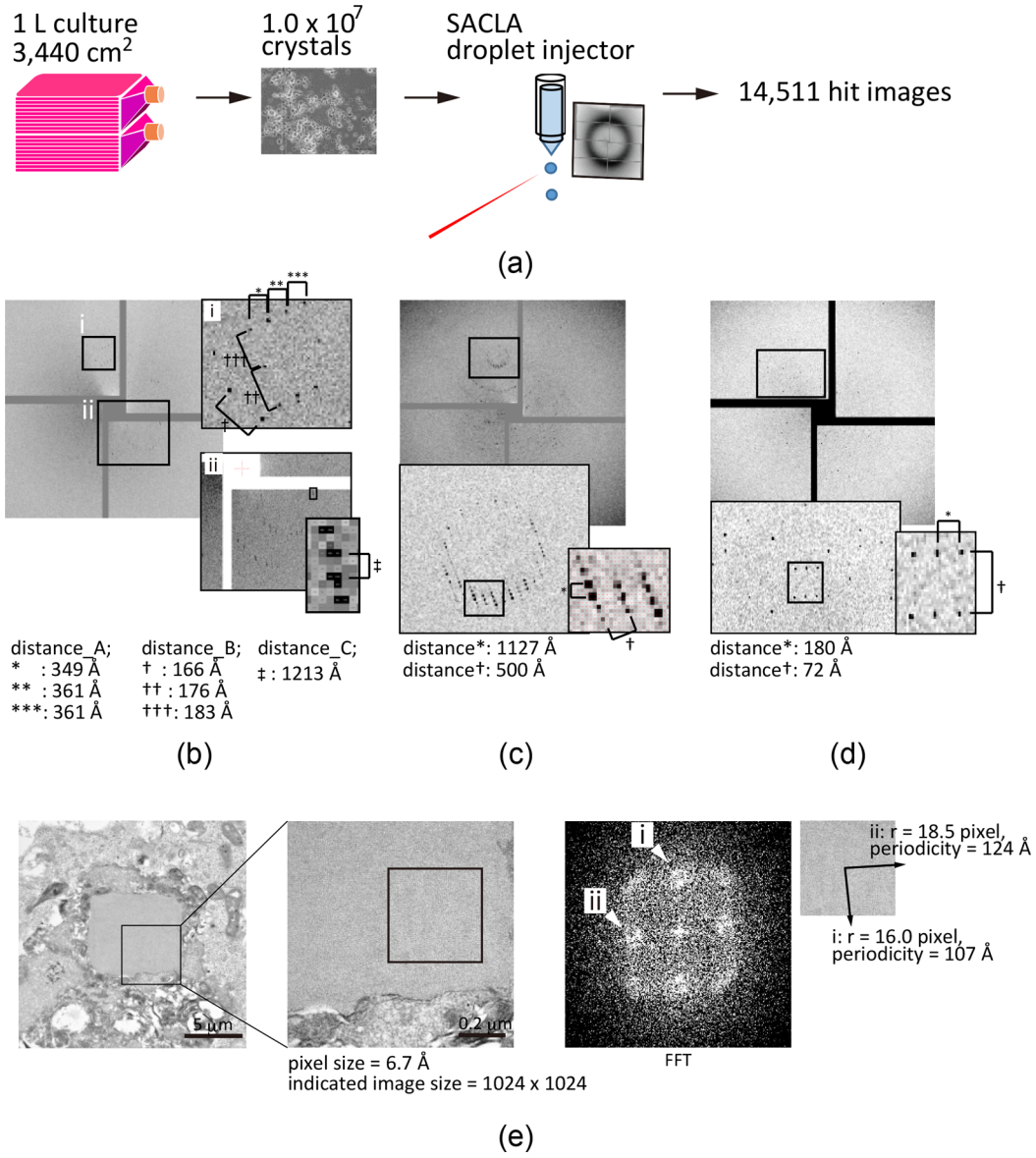

Figure 5. XFEL analyses of NEU1 *in cellulo* crystals. (a) Summary of this experiment. Cells cultured in 1 L medium in a Corning Hyperflask M were transported to SACLA. Just before the beamtime, 1.0×10^7 crystals were extracted and delivered by a droplet injector, and XFEL diffraction images were obtained. When a 6 h beamtime was used, 14,511 diffraction images were obtained through the Cheetah- and CrystFEL-based pipeline in SACLA.[34] The image of the extracted crystals is the same as in Figure 3d. (b–d) Representative diffraction images of the NEU1 crystals. The indicated regions were enlarged, and the distance of the spots was measured with Adxv. The enlarged images were captured with Adxv and reflected vertically. The images often contained diffraction spots in close proximity to each other (b, c). Some images similar to the one shown in the previous study[27] were also observed. (e) Crystals showing a characteristic pattern. The cell was dying, and its nucleus was no longer unclear. The region shown in the square (left panel) is enlarged in the right panel. The image of the enlarged region was FFT using ImageJ2. On the FFT image, periodicities of the TEM image were calculated. Periodicities of 107 Å in the direction of "*i*" and 124 Å in the direction of "*ii*" were calculated. The angle between the directions of "*i*" and "*ii*" was approximately 95°.

Our first goal was to execute an SFX experiment with a sufficient number of the extracted *in cellulo* crystals. Since Western blotting analysis revealed a correlation between protein production and the quantity of crystals, we reasoned that the protein production level would be a key parameter for increasing the number of *in cellulo* crystals. To increase the protein production, a retransfection method was applied. Our results showed that the retransfection enhanced the NEU1 protein production, resulting in 6 times as many crystals as by the transient transfection. The increased number of crystals resulted in fewer cultured cells, which had the benefit that the ratio of the extracted crystals to the cell debris became much higher. This was critical for maintaining a high hit rate in SFX experiments.

Gallat et al. obtained only a single diffraction image with 3 Å resolution.[27] Our 14,511 images indicated that NEU1 *in cellulo* crystals in the study diffracted to 8 Å. The low quality of the crystals was consistent with the results of FFT analysis of a TEM image. Although the NEU1 *in cellulo* crystallization did not lead to the crystal structure due to the low quality of the crystals, the study shed light on the characteristics of NEU1 crystals and suggested a way to improve the production and extraction of crystals. Since 2385 proteins including membrane proteins in the rat liver were identified as lysosomal proteins,[48] the *in cellulo*

DOI: 10.1021/acsabm.9b00686
ACS Appl. Bio Mater. 2019, 2, 4941–4952

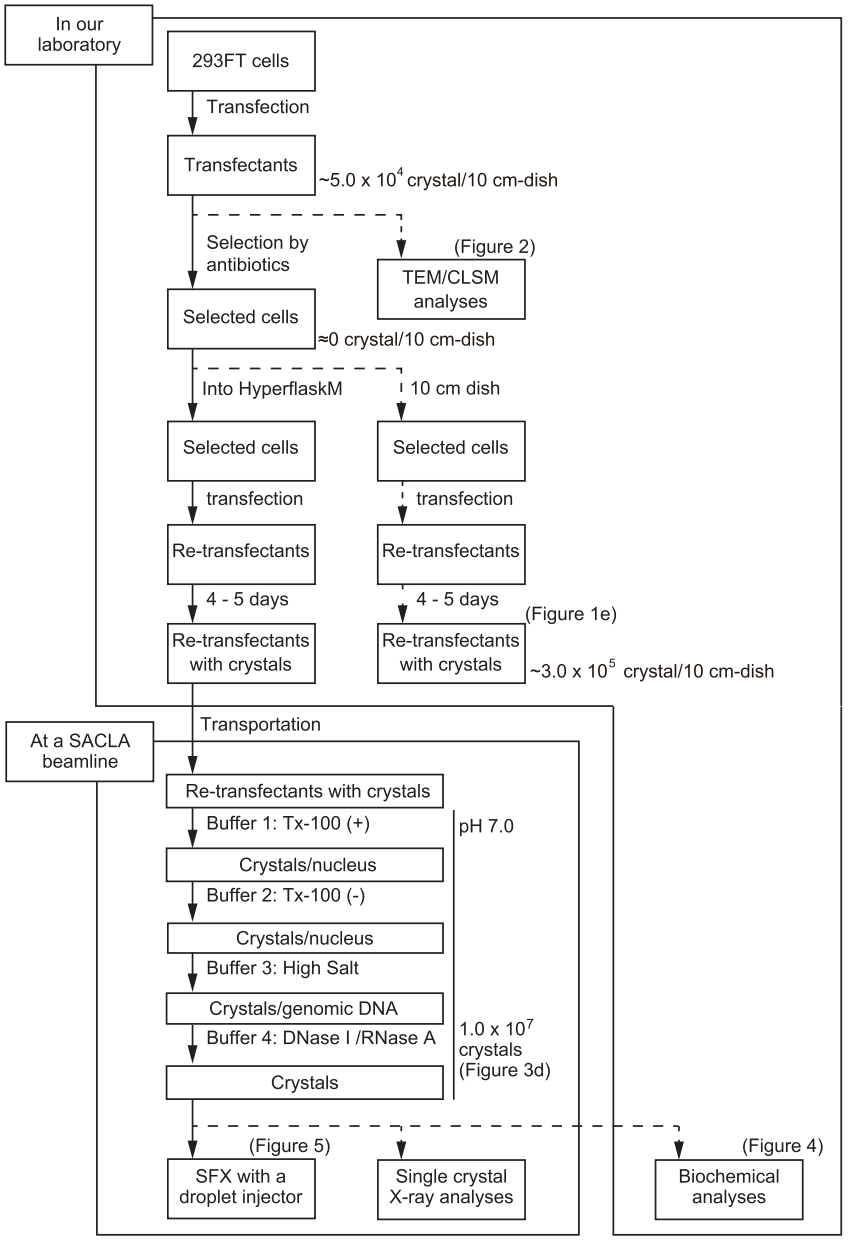

Figure 6. Scheme of NEU1 *in cellulo* crystallography. The scheme of the NEU1 *in cellulo* crystallography method is shown. Arrows with continuous lines indicate the main procedures for the SFX experiment, and arrows with dotted lines represent additional procedures for quality control experiments or for biochemical analyses. NEU1 *in cellulo* crystals were prepared in the KEK and transported to the SACLA beamline. Just before the beamtime, the *in cellulo* crystals were extracted at the beamline. Crucial components are indicated, namely, 0.1% Triton X-100 (Tx-100) for Buffer 1 to lyse cells and 1.0 M NaCl (high salt) for Buffer 3 to disrupt the nuclei. To maintain unsolubilized NEU1 *in cellulo* crystals, the buffers were kept at pH 7.0. In this study, single crystal X-ray analyses were not performed.

crystallization method can be tested on other lysosomal proteins with unknown structures. If we could improve not only the quantity but also the quality of the *in cellulo* crystals by optimizations like those performed in this study, then *in cellulo* crystallography might become a practical tool for use in conjunction with conventional *in vitro* protein crystallization, because the protein purification and crystallization screening steps are not required.

■ ASSOCIATED CONTENT

Supporting Information

The Supporting Information is available free of charge on the ACS Publications website at DOI: 10.1021/acsabm.9b00686.

Table S1: Cell lines used in this study. Figure S1: A diffraction image of a NEU1 crystal taken using synchrotron radiation. Figure S2: Expression of NEU1_N352A in 293FT cells (PDF)

■ AUTHOR INFORMATION

Corresponding Authors

*E-mail: fumiaki.yumoto1@gmail.com. Phone: +81-29-879-6176. Fax: +81-29-879-6179.

*E-mail: kitoh@tokushima-u.ac.jp. Phone and fax: +81-88-633-7290.

ORCID

Kotaro Koiwai: 0000-0002-9684-3699

DOI: 10.1021/acsabm.9b00686
ACS Appl. Bio Mater. 2019, 2, 4941−4952

Fumitaka Mafuné: 0000-0001-8860-6354

Author Contributions

K.K., J.T., L.M.G.C., R.K., T.S., K.I., and F.Y. designed the research. K.K., J.T., T.H., and F.Y. performed biochemical assays. F.M., K.M., M.S., T.T., K.T., Y.J., M.Y., T.N., E.N., and S.I. established experimental apparatus and the conditions for SFX experiments. K.K, J.T., N.M., S.S., A.J., M.S., T.T., E.M., T.N., E.N., L.M.G.C., and F.Y. performed the SFX experiments. M.W., O.N., S.I, T.S., and K.I. advised and supervised the members. K.K., M.N., and T.N. analyzed SFX data. K.K., T.S., and F.Y. wrote the manuscript. All authors gave their approval to the final version.

Notes

The authors declare no competing financial interest.

■ ACKNOWLEDGMENTS

We thank Rie Tanaka for administrative assistance with the SACLA SFX experiment and Elena Sablin for critical reading. TEM data analyses were supported by Naruhiko Adachi. This research was supported by the Platform Project for Supporting in Drug Discovery and Life Science Research (Platform for Drug Discovery, Informatics, and Structural Life Science: PDIS) and Basis for Supporting Innovative Drug Discovery and Life Science Research from the Japan Agency for Medical Research and Development (AMED). The XFEL experiments were carried out at the BL3 of SACLA with the approval of the Japan Synchrotron Radiation Research Institute (JASRI) (proposal no. 2015B8048). The synchrotron experiment was carried out at the BL41XU of SPring-8 supported by the PDIS. This work was supported by the X-ray Free-Electron Laser Priority Strategy Program (MEXT) and JSPS KAKENHI grant number JP16K18507. We acknowledge computational support from the SACLA HPC system and Mini-K super computer system. This work was performed under the approval of the Photon Factory Program Advisory Committee (proposal no. 2016G167).

■ ABBREVIATIONS

XFEL, X-ray free electron laser; SACLA, SPring-8 Å Compact Free Electron Laser; SFX, serial femtosecond crystallography; NEU1, neuraminidase-1; HEK, human embryonic kidney; ER, endoplasmic reticulum; TEM, transmission electron microscopy; FFT, fast Fourier-transform.

■ REFERENCES

(1) Schönherr, R.; Rudolph, J. M.; Redecke, L. Protein Crystallization in Living Cells. *Biol. Chem.* **2018**, *399* (7), 751−772.

(2) Charcot, J.-M. C. R. Observation de Leucocythémie. *C. R. Seances Soc. Biol.* **1853**, *5*, 44−50.

(3) Cornalia, E. *Monografia Del Bombice Del Gelso (Bombix Mori Linn.)*; Giuseppe Bernardoni: Milano, 1856.

(4) Maestri, A. Del Giallume. In *Frammenti Anatomici Fisiologici e Patologici Sul Baco Da Seta*; Fusi: Pavia, 1856.

(5) Leonidas, D. D.; Elbert, B. L.; Zhou, Z.; Leffler, H.; Ackerman, S. J.; Acharya, K. R. Crystal Structure of Human Charcot-Leyden Crystal Protein, an Eosinophil Lysophospholipase, Identifies It as a New Member of the Carbohydrate-Binding Family of Galectins. *Structure* **1995**, *3* (12), 1379−1393.

(6) Coulibaly, F.; Chiu, E.; Ikeda, K.; Gutmann, S.; Haebel, P. W.; Schulze-Briese, C.; Mori, H.; Metcalf, P. The Molecular Organization of Cypovirus Polyhedra. *Nature* **2007**, *446* (7131), 97−101.

(7) Glaser, R. W.; Chapman, J. W. The Wilt Disease of Gipsy Moth Caterpillars1. *J. Econ. Entomol.* **1913**, *6*, 479.

(8) Levin-Zaidman, S.; Frenkiel-Krispin, D.; Shimoni, E.; Sabanay, I.; Wolf, S. G.; Minsky, a. Ordered Intracellular RecA-DNA Assemblies: A Potential Site of in Vivo RecA-Mediated Activities. *Proc. Natl. Acad. Sci. U. S. A.* **2000**, *97* (12), 6791−6796.

(9) Sawaya, M. R.; Cascio, D.; Gingery, M.; Rodriguez, J.; Goldschmidt, L.; Colletier, J.-P.; Messerschmidt, M. M.; Boutet, S.; Koglin, J. E.; Williams, G. J.; Brewster, A. S.; Nass, K.; Hattne, J.; Botha, S.; Doak, R. B.; Shoeman, R. L.; DePonte, D. P.; Park, H. W.; Federici, B.; Sauter, N. K.; Schlichting, I.; Eisenberg, D. S. Protein Crystal Structure Obtained at 2.9 Å Resolution from Injecting Bacterial Cells into an X-Ray Free-Electron Laser Beam. *Proc. Natl. Acad. Sci. U. S. A.* **2014**, *111* (35), 12769−12774.

(10) Vayssié, L.; Skouri, F.; Sperling, L.; Cohen, J. Molecular Genetics of Regulated Secretion in Paramecium. *Biochimie* **2000**, *82* (4), 269−288.

(11) Veenhuis, M.; van Dijken, J. P.; Pilon, S. A. F.; Harder, W. Development of Crystalline Peroxisomes in Methanol-Grown Cells of the Yeast Hansenula Polymorpha and Its Relation to Environmental Conditions. *Arch. Microbiol.* **1978**, *117* (2), 153−163.

(12) Jakobi, A. J.; Passon, D. M.; Knoops, K.; Stellato, F.; Liang, M.; White, T. A.; Seine, T.; Messerschmidt, M.; Chapman, H. N.; Wilmanns, M. In Cellulo Serial Crystallography of Alcohol Oxidase Crystals inside Yeast Cells. *IUCrJ* **2016**, *3*, 88−95.

(13) Banerjee, S.; Coussens, N. P.; Gallat, F.-X.; Sathyanarayanan, N.; Srikanth, J.; Yagi, K. J.; Gray, J. S. S.; Tobe, S. S.; Stay, B.; Chavas, L. M. G.; Ramaswamy, S. Structure of a Heterogeneous, Glycosylated, Lipid-Bound, *in Vivo* -Grown Protein Crystal at Atomic Resolution from the Viviparous Cockroach *Diploptera Punctata*. *IUCrJ* **2016**, *3* (4), 282−293.

(14) Giembycz, M. a.; Lindsay, M. a. Pharmacology of the Eosinophil. *Pharmacol. Rev.* **1999**, *51* (2), 213−340.

(15) Koopmann, R.; Cupelli, K.; Redecke, L.; et al. In Vivo Protein Crystallization Opens New Routes in Structural Biology. *Nat. Methods* **2012**, *9* (3), 259−262.

(16) Duszenko, M.; Redecke, L.; Mudogo, C. N.; Sommer, B. P.; Mogk, S.; Oberthuer, D.; Betzel, C. In Vivo Protein Crystallization in Combination with Highly Brilliant Radiation Sources Offers Novel Opportunities for the Structural Analysis of Post-Translationally Modified Eukaryotic Proteins. *Acta Crystallogr., Sect. F: Struct. Biol. Commun.* **2015**, *71*, 929−937.

(17) Boudes, M.; Garriga, D.; Fryga, A.; Caradoc-Davies, T.; Coulibaly, F. A Pipeline for Structure Determination of *in Vivo* -Grown Crystals Using *in Cellulo* Diffraction. *Acta Crystallographica Section D Structural Biology* **2016**, *72* (4), 576−585.

(18) Hasegawa, H.; Wendling, J.; He, F.; Trilisky, E.; Stevenson, R.; Franey, H.; Kinderman, F.; Li, G.; Piedmonte, D. M.; Osslund, T.; Shen, M.; Ketchem, R. R. In Vivo Crystallization of Human IgG in the Endoplasmic Reticulum of Engineered Chinese Hamster Ovary (CHO) Cells. *J. Biol. Chem.* **2011**, *286* (22), 19917−19931.

(19) Tsutsui, H.; Jinno, Y.; Shoda, K.; Tomita, A.; Matsuda, M.; Yamashita, E.; Katayama, H.; Nakagawa, A.; Miyawaki, A. A Diffraction-Quality Protein Crystal Processed as an Autophagic Cargo. *Mol. Cell* **2015**, *58* (1), 186−193.

(20) Baskaran, Y.; Ang, K. C.; Anekal, P. V.; Chan, W. L.; Grimes, J. M.; Manser, E.; Robinson, R. C. An in Cellulo-Derived Structure of PAK4 in Complex with Its Inhibitor Inka1. *Nat. Commun.* **2015**, *6* (May), 8681.

(21) Abe, S.; Tabe, H.; Ijiri, H.; Yamashita, K.; Hirata, K.; Atsumi, K.; Shimoi, T.; Akai, M.; Mori, H.; Kitagawa, S.; Ueno, T. Crystal Engineering of Self-Assembled Porous Protein Materials in Living Cells. *ACS Nano* **2017**, *11*, 2410.

(22) Bonten, E.; Van Der Spoel, A.; Fornerod, M.; Grosveld, G.; D'Azzo, A. Characterization of Human Lysosomal Neuraminidase Defines the Molecular Basis of the Metabolic Storage Disorder Sialidosis. *Genes Dev.* **1996**, *10* (24), 3156−3169.

(23) Monti, E.; Bonten, E.; D'Azzo, A.; Bresciani, R.; Venerando, B.; Borsani, G.; Schauer, R.; Tettamanti, G.. Sialidases in Vertebrates: A Family Of Enzymes Tailored For Several Cell Functions. *Advances in*

DOI: 10.1021/acsabm.9b00686
ACS Appl. Bio Mater. 2019, 2, 4941−4952

Carbohydrate Chemistry and Biochemistry; Academic Press: Cambridge, MA, 2010; Vol. *64*, pp 403−479.
(24) Van Der Spoel, A.; Bonten, E.; D'Azzo, A. Transport of Human Lysosomal Neuraminidase to Mature Lysosomes Requires Protective Protein/Cathepsin A. *EMBO J.* **1998**, *17* (6), 1588−1597.
(25) Oohira, T.; Nagata, N.; Akaboshi, I.; Matsuda, I.; Naito, S. The Infantile Form of Sialidosis Type II Associated with Congenital Adrenal Hyperplasia: Possible Linkage between HLA and the Neuraminidase Deficiency Gene. *Hum. Genet.* **1985**, *70* (4), 341−343.
(26) Loonen, M. C. B.; Reuser, A. J. J.; Visser, P.; Arts, W. F. M. Combined Sialidase (Neuraminidase) and P-Galactosidase Deficiency. Clinical, Morphological and Enzymological Observations in a Patient. *Clin. Genet.* **1984**, *26* (2), 139−149.
(27) Gallat, F.-X.; Matsugaki, N.; Coussens, N. P.; Yagi, K. J.; Boudes, M.; Higashi, T.; Tsuji, D.; Tatano, Y.; Suzuki, M.; Mizohata, E.; Tono, K.; Joti, Y.; Kameshima, T.; Park, J.; Song, C.; Hatsui, T.; Yabashi, M.; Nango, E.; Itoh, K.; Coulibaly, F.; Tobe, S.; Ramaswamy, S.; Stay, B.; Iwata, S.; Chavas, L. M. G. In Vivo Crystallography at X-Ray Free-Electron Lasers: The next Generation of Structural Biology? *Philos. Trans. R. Soc., B* **2014**, *369* (1647), 20130497−20130497.
(28) Schindelin, J.; Rueden, C. T.; Hiner, M. C.; Eliceiri, K. W. The ImageJ Ecosystem: An Open Platform for Biomedical Image Analysis. *Mol. Reprod. Dev.* **2015**, *82* (7−8), 518−529.
(29) Tono, K.; Togashi, T.; Inubushi, Y.; Sato, T.; Katayama, T.; Ogawa, K.; Ohashi, H.; Kimura, H.; Takahashi, S.; Takeshita, K.; Tomizawa, H.; Goto, S.; Ishikawa, T.; Yabashi, M. Beamline, Experimental Stations and Photon Beam Diagnostics for the Hard x-Ray Free Electron Laser of SACLA. *New J. Phys.* **2013**, *15* (8), 083035.
(30) Mafune, F.; Miyajima, K.; Tono, K.; Takeda, Y.; Kohno, J.; Miyauchi, N.; Kobayashi, J.; Joti, Y.; Nango, E.; Iwata, S.; Yabashi, M. Microcrystal Delivery by Pulsed Liquid Droplet for Serial Femtosecond Crystallography. *Acta Crystallogr. D: Struct. Biol.* **2016**, *72*, 520−523.
(31) Tono, K.; Nango, E.; Sugahara, M.; Song, C.; Park, J.; Tanaka, T.; Tanaka, R.; Joti, Y.; Kameshima, T.; Ono, S.; Hatsui, T.; Mizohata, E.; Suzuki, M.; Shimamura, T.; Tanaka, Y.; Iwata, S.; Yabashi, M. Diverse Application Platform for Hard X-Ray Diffraction in SACLA (DAPHNIS): Application to Serial Protein Crystallography Using an X-Ray Free-Electron Laser. *J. Synchrotron Radiat.* **2015**, *22*, 532−537.
(32) Kameshima, T.; Ono, S.; Kudo, T.; Ozaki, K.; Kirihara, Y.; Kobayashi, K.; Inubushi, Y.; Yabashi, M.; Horigome, T.; Holland, A.; Holland, K.; Burt, D.; Murao, H.; Hatsui, T. Development of an X-Ray Pixel Detector with Multi-Port Charge-Coupled Device for X-Ray Free-Electron Laser Experiments. *Rev. Sci. Instrum.* **2014**, *85* (3), 033110.
(33) Barty, A.; Kirian, R. A.; Maia, F. R. N. C.; Hantke, M.; Yoon, C. H.; White, T. A.; Chapman, H. Cheetah: Software for High-Throughput Reduction and Analysis of Serial Femtosecond X-Ray Diffraction Data. *J. Appl. Crystallogr.* **2014**, *47* (3), 1118−1131.
(34) Nakane, T.; Joti, Y.; Tono, K.; Yabashi, M.; Nango, E.; Iwata, S.; Ishitani, R.; Nureki, O. Data Processing Pipeline for Serial Femtosecond Crystallography at SACLA. *J. Appl. Crystallogr.* **2016**, *49* (3), 1035.
(35) Duisenberg, A. J. M. Indexing in Single-Crystal Diffractometry with an Obstinate List of Reflections. *J. Appl. Crystallogr.* **1992**, *25*, 92−96.
(36) White, T. A.; Kirian, R. A.; Martin, A. V.; Aquila, A.; Nass, K.; Barty, A.; Chapman, H. N. CrystFEL: A Software Suite for Snapshot Serial Crystallography. *J. Appl. Crystallogr.* **2012**, *45* (2), 335−341.
(37) Johansson, L. C.; Stauch, B.; Ishchenko, A.; Cherezov, V. A Bright Future for Serial Femtosecond Crystallography with XFELs. *Trends Biochem. Sci.* **2017**, *42* (9), 749−762.
(38) Shimmoto, M.; Fukuhara, Y.; Itoh, K.; Oshima, A.; Sakuraba, H.; Suzuki, Y. Protective Protein Gene Mutations in Galactosialidosis. *J. Clin. Invest.* **1993**, *91* (6), 2393−2398.
(39) Oheda, Y.; Kotani, M.; Murata, M.; Sakuraba, H.; Kadota, Y.; Tatano, Y.; Kuwahara, J.; Itoh, K. Elimination of Abnormal Sialylglycoproteins in Fibroblasts with Sialidosis and Galactosialidosis by Normal Gene Transfer and Enzyme Replacement. *Glycobiology* **2006**, *16* (4), 271−280.
(40) Ueki, S.; Tokunaga, T.; Melo, R. C. N.; Saito, H.; Honda, K.; Fukuchi, M.; Konno, Y.; Takeda, M.; Yamamoto, Y.; Hirokawa, M.; Fujieda, S.; Spencer, L. A.; Weller, P. F. Charcot-Leyden Crystal Formation Is Closely Associated with Eosinophil Extracellular Trap Cell Death. *Blood* **2018**, *132* (20), 2183−2187.
(41) Johnson, D. E.; Ostrowski, P.; Jaumouillé, V.; Grinstein, S. The Position of Lysosomes within the Cell Determines Their Luminal PH. *J. Cell Biol.* **2016**, *212* (6), 677−692.
(42) Ahluwalia, N.; Bergeron, J. J. M.; Wada, I.; Degen, E.; Williams, D. B. The P88 Molecular Chaperone Is Identical to the Endoplasmic Reticulum Membrane Protein, Calnexin. *J. Biol. Chem.* **1992**, *267* (15), 10914−10918.
(43) Chen, J. W.; Cha, Y.; Yukselq, K. U.; Gracyq, R. W.; August, J. T. Isolation and Sequencing of a CDNA Clone Encoding Lysosomal Membrane Glycoprotein Mouse LAMP- 1. *J. Biol. Chem.* **1988**, *263* (18), 8754−8758.
(44) Hasegawa, H. Simultaneous Induction of Distinct Protein Phase Separation Events in Multiple Subcellular Compartments of a Single Cell. *Exp. Cell Res.* **2019**, *379*, 92.
(45) Kim, J. H.; Johannes, L.; Goud, B.; Antony, C.; Lingwood, C. A.; Daneman, R.; Grinstein, S. Noninvasive Measurement of the PH of the Endoplasmic Reticulum at Rest and during Calcium Release. *Proc. Natl. Acad. Sci. U. S. A.* **1998**, *95* (6), 2997−3002.
(46) Yang, X.; Liu, F.; Yan, Y.; Zhou, T.; Guo, Y.; Sun, G.; Zhou, Z.; Zhang, W.; Guo, X.; Sha, J. Proteomic Analysis of N-Glycosylation of Human Seminal Plasma. *Proteomics* **2015**, *15* (7), 1255−1258.
(47) Senda, M.; Hayashi, T.; Hatakeyama, M.; Takeuchi, K.; Sasaki, A. T.; Senda, T. Use of Multiple Cryoprotectants to Improve Diffraction Quality from Protein Crystals. *Cryst. Growth Des.* **2016**, *16* (3), 1565−1571.
(48) Chapel, A.; Kieffer-Jaquinod, S.; Sagne, C.; Verdon, Q.; Ivaldi, C.; Mellal, M.; Thirion, J.; Jadot, M.; Bruley, C.; Garin, J.; Gasnier, B.; Journet, A. An Extended Proteome Map of the Lysosomal Membrane Reveals Novel Potential Transporters. *Mol. Cell. Proteomics* **2013**, *12* (6), 1572−1588.

DOI: 10.1021/acsabm.9b00686
ACS Appl. Bio Mater. 2019, 2, 4941−4952